Increased ATPase activity produced by mutations at arginine-1380 in nucleotide-binding domain 2 of *ABCC8* causes neonatal diabetes

Heidi de Wet*, Mathew G. Rees*, Kenju Shimomura*, Jussi Aittoniemi*†, Ann-Marie Patch‡, Sarah E. Flanagan‡, Sian Ellard‡, Andrew T. Hattersley‡, Mark S. P. Sansom†, and Frances M. Ashcroft*§

*Henry Wellcome Centre for Gene Function, Department of Physiology, Anatomy and Genetics, University of Oxford, Parks Road, Oxford OX1 3PT, United Kingdom; †Department of Biochemistry, University of Oxford, South Parks Road, Oxford OX1 3QU, United Kingdom; and ‡Institute of Biomedical and Clinical Science, Peninsula Medical School, Exeter EX2 5DW, United Kingdom

Edited by Christopher Miller, Brandeis University, Waltham, MA, and approved October 3, 2007 (received for review August 7, 2007)

Gain-of-function mutations in the genes encoding the ATP-sensitive potassium (K_{ATP}) channel subunits Kir6.2 (*KCNJ11*) and SUR1 (*ABCC8*) are a common cause of neonatal diabetes mellitus. Here we investigate the molecular mechanism by which two heterozygous mutations in the second nucleotide-binding domain (NBD2) of SUR1 (R1380L and R1380C) separately cause neonatal diabetes. SUR1 is a channel regulator that modulates the gating of the pore formed by Kir6.2. K_{ATP} channel activity is inhibited by ATP binding to Kir6.2 but is stimulated by MgADP binding, or by MgATP binding and hydrolysis, at the NBDs of SUR1. Functional analysis of purified NBD2 showed that each mutation enhances MgATP hydrolysis by purified isolated fusion proteins of maltose-binding protein and NBD2. Inhibition of ATP hydrolysis by MgADP was unaffected by mutation of R1380, but inhibition by beryllium fluoride (which traps the ATPase cycle in the prehydrolytic state) was reduced. MgADP-dependent activation of K_{ATP} channel activity was unaffected. These data suggest that the R1380L and R1380C mutations enhance the off-rate of P_i, thereby enhancing the hydrolytic rate. Molecular modeling studies supported this idea. Because mutant channels were inhibited less strongly by MgATP, this would increase K_{ATP} currents in pancreatic beta cells, thus reducing insulin secretion and producing diabetes.

SUR1 | K_{ATP} channel | ATP hydrolysis | sulfonylurea receptor

Activating mutations in the *ABCC8* and *KCNJ11* genes are a common cause of neonatal diabetes (1–3). *ABCC8* encodes the regulatory subunit of the ATP-sensitive potassium (K_{ATP}) channel. It coassembles with pore-forming Kir6.2 (*KCNJ11*) subunits to form an octameric channel, with a central tetrameric Kir6.2 pore being surrounded by four SUR1 subunits (4). Both Kir6.2 and SUR1 serve as metabolic sensors, enabling the K_{ATP} channel to respond to changes in cellular metabolism. In addition, SUR1 endows the channel with sensitivity to the antidiabetic sulfonylurea drugs.

In pancreatic beta cells, metabolic regulation of K_{ATP} channels is crucial for glucose-stimulated insulin secretion (Fig. 1*A*) (3). In unstimulated cells, K_{ATP} channels are open and hyperpolarize the membrane enough to keep voltage-gated Ca^{2+} channels closed. When the plasma glucose concentration rises, glucose uptake and metabolism by the beta cell are enhanced, leading to K_{ATP} channel closure. This causes a membrane depolarization that triggers opening of voltage-gated Ca^{2+} channels and Ca^{2+}-dependent electrical activity. The consequent Ca^{2+} influx stimulates insulin release.

Metabolic regulation of K_{ATP} channel activity is mediated by changes in the concentration of adenine nucleotides, which interact with both Kir6.2 and SUR1 subunits. Binding of ATP to Kir6.2, in a Mg-independent fashion, shuts the channel (5). In contrast, MgADP binding to SUR1 stimulates channel opening (5, 6). Although MgATP can also stimulate K_{ATP} channel activity by interaction with SUR1 (7) it must first be hydrolyzed to MgADP (8). K_{ATP} channel activity is thus governed by the balance between the inhibitory and stimulatory effects of nucleotides, with low metabolism (low ATP, high MgADP) favoring channel activation and high metabolism (high ATP, low MgADP) favoring inhibition (Fig. 1*A*).

Here we report a functional mechanism for neonatal diabetes, caused by two different mutations at SUR1 residue 1380, which lies within the second nucleotide-binding domain (NBD2) (9, 10). Our results show that mutation of R1380 to leucine or cysteine results in increased ATPase activity at NBD2. This increase reduces the sensitivity of the channel to inhibition by MgATP and increases the whole-cell K_{ATP} current. In pancreatic beta cells, a similar increase in K_{ATP} current would be expected to impair insulin secretion and thereby cause diabetes.

Results

Molecular Genetic Analysis. The R1380C mutation (c.4138C>T) has been reported in three probands with transient neonatal diabetes (9, 10). Two mutations had arisen *de novo*, but in the other family there was a family history of adult-onset type 2 diabetes or gestational diabetes in mutation carriers. Two pedigrees with the R1380L mutation (c.4139G>T) were identified. The probands and a sibling had diabetes during the neonatal period but inherited the mutation from a parent/grandparent diagnosed with diabetes in adulthood (at 19, 22, 25, and 30 years of age).

Arginine-1380 lies immediately upstream of the Walker A motif of NBD2, which has been implicated in the hydrolysis of MgATP. It is highly conserved and found in the NBD2 of all members of the ABCC subfamily of ATP-binding cassette (ABC) proteins (Fig. 1*B*), but has not been previously implicated in nucleotide binding or hydrolysis.

ATPase Activity. Wild-type NBD2 hydrolyzed ATP with a maximal turnover rate (k_{cat}) of 0.08 s^{-1} and a K_m of 0.41 mM (Fig. 2*A* and Table 1). The latter is within the range reported previously [0.35–0.6 mM (11, 12)]. Mutation of R1380 to cysteine or leucine did not significantly alter the K_m but increased k_{cat} by 1.2-fold ($P < 0.05$) and 1.7-fold ($P < 0.01$), respectively (Fig. 2*A* and Table 1).

In all ABC proteins that have been studied, NBD1 and NBD2

Author contributions: H.d.W., M.S.P.S., and F.M.A. designed research; H.d.W., M.G.R., K.S., and J.A. performed research; A.-M.P., S.E.F., S.E., and A.T.H. contributed new reagents/analytic tools; H.d.W. and K.S. analyzed data; and H.d.W. and F.M.A. wrote the paper.

The authors declare no conflict of interest.

This article is a PNAS Direct Submission.

§To whom correspondence should be addressed. E-mail: frances.ashcroft@physiol.ox.ac.uk.

This article contains supporting information online at www.pnas.org/cgi/content/full/0707428104/DC1.

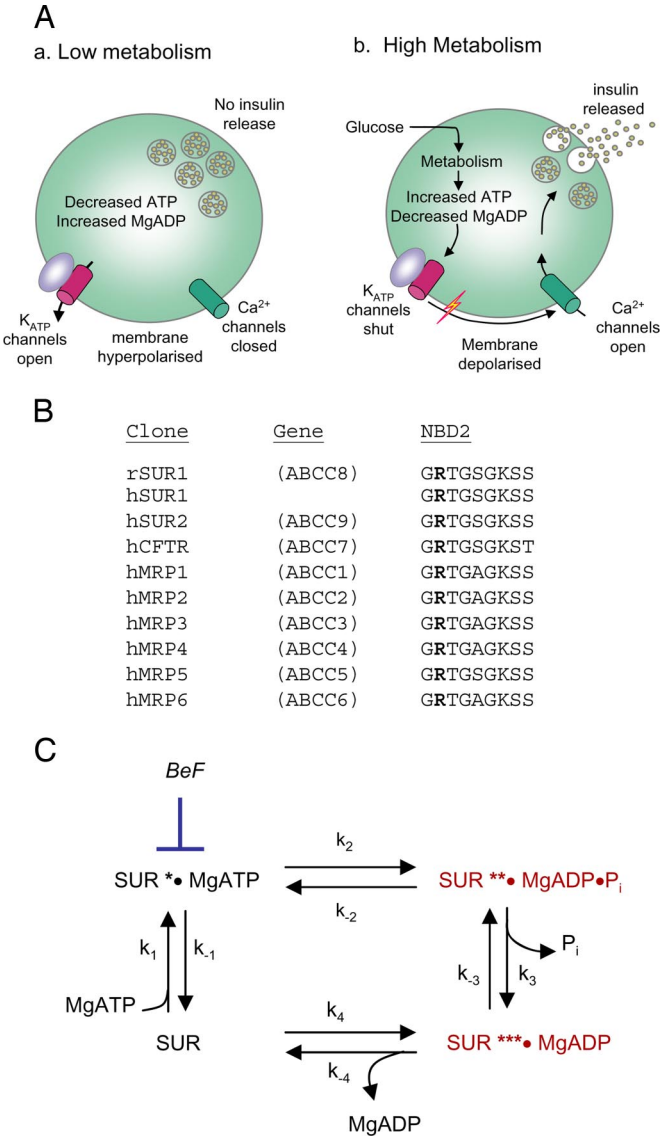

Fig. 1. Function and mechanism of the NBDs of SUR1. (*A*) Role of the K_{ATP} channel in glucose-stimulated insulin secretion. (*B*) Comparison of the amino acid sequences of the Walker A motifs (consensus: GXXXXGKT/S) in the NBDs of various ABCC-family proteins. Residues equivalent to SUR1-R1380 are in boldface. MRP, multidrug resistance-related protein; CFTR, cystic fibrosis transmembrane conductance regulator. (*C*) The SUR1 ATPase catalytic cycle. BeF, beryllium fluoride (BeF_3^- and BeF_4^{2-}).

associate in a sandwich dimer conformation to form two catalytic ATP-binding sites (site 1 and site 2). These each contain residues from the Walker A and Walker B motifs of one NBD and from the signature sequence of the other NBD (13–16). In our studies, NBD2 will associate as a homodimer. As previously reported (12), mixing wild-type NBD1 and NBD2 did not appear to affect the catalytic activity of either NBD [supporting information (SI) Tables 3 and 4]. Furthermore, both the R1380L and the R1380C mutations increased the ATPase activity of the NBD1–NBD2 mixture (SI Table 3).

Previous studies have shown that MgADP acts as a competitive inhibitor of ATP hydrolysis at NBD2 by trapping the ATPase cycle in the posthydrolytic conformation (Fig. 1*C*) (8, 12). The nucleotide inhibited ATP hydrolysis by wild-type NBD2 with a K_i of 0.85 mM (Fig. 2*B* and Table 2). K_i values for the R1380C and R1380L mutants were not significantly different from those of the wild type. There was also no effect of the mutation on MgADP inhibition of ATPase activity when wild-type NBD1 was mixed with wild-type or mutant NBD2 (SI Table 5).

Beryllium fluoride (BeF_3^- and BeF_4^{2-}, abbreviated here as BeF) is a potent inhibitor of ATP hydrolysis by many ABC proteins, including the isolated NBD2 of SUR1 and SUR2 (8, 12). It acts by arresting the ATPase cycle in the prehydrolytic conformation (Fig. 1*C*) (17). The ATPase activity of wild-type NBD2 was potently inhibited by BeF with a K_i of 20 μM, as previously reported (19 μM in ref. 12). Both mutants were significantly less blocked by BeF, the K_i being increased 2.5-fold for R1380C and 5-fold for R1380L (Fig. 2*C* and Table 2).

K_{ATP} Currents. We next examined the effect of mutating R1380 on K_{ATP} currents, by coexpressing wild-type or mutant SUR1 with Kir6.2. We focused on the R1380L mutation, which shows the greatest reduction in ATP hydrolysis.

Fig. 3 shows that whole-cell K_{ATP} currents are very small under resting conditions, presumably because of the high intracellular ATP concentration, but are dramatically increased by sodium azide, which inhibits mitochondrial metabolism. Resting R1380L currents were slightly (2-fold), but significantly ($P < 0.01$), larger than wild type. They were further increased by metabolic inhibition, indicating that the channel is only partially closed at resting ATP. The sulfonylurea tolbutamide blocked wild-type currents by 96 ± 1% ($n = 12$) and R1380L currents by 87 ± 5% ($n = 13$) ($P < 0.05$) (Fig. 3). This finding suggests that the diabetes of patients carrying these mutations should be treatable with sulfonylureas.

As Fig. 4*A* shows, R1380L channels were less ATP sensitive than wild type, when measured in inside-out patches. The concentration of ATP causing half-maximal block (IC_{50}) increased from 16 μM to 35 μM when R1380 was mutated (SI Table 6). Furthermore, the amount of current that remained unblocked at physiological MgATP concentrations (1–10 mM) increased from <1% of maximal for wild-type channels to 5% for R1380L channels at 3 mM MgATP.

Although ATP is thought to influence K_{ATP} channel activity in Mg^{2+}-free solutions only via Kir6.2, the ATP sensitivity of the mutant channel in the absence of Mg^{2+} also differed from that of wild type (Fig. 4*B*). The IC_{50} increased ≈3-fold, from 5 μM to 16 μM (Fig. 4*B*, SI Table 6). The intrinsic open probability (P_o) (i.e., that measured in the absence of nucleotide) was unaffected by the mutation, being 0.21 ± 0.03 ($n = 8$) for wild-type compared with 0.28 ± 0.06 ($n = 6$) for R1380L channels. These results contrast with some other SUR1 ND mutations, which reduce the ATP sensitivity of the K_{ATP} channel in Mg^{2+}-free solutions by impairing gating (18).

Finally, no significant difference was observed in the extent of channel activation by MgADP in either the presence or absence of ATP (Fig. 5), consistent with the fact that the K_i for MgADP inhibition of ATP hydrolysis remained unchanged (Fig. 2*B*).

Structural Considerations. The three-dimensional structure of SUR1 at atomic resolution is unknown. However, crystal structures of the NBDs of many ABC proteins have been solved (14–16). These all share the same overall fold, suggesting that homology models based on these structures may provide a reasonable approximation to the backbone structure of SUR1.

A homology model of the NBD heterodimer of SUR1 based on the crystal structure of Sav1866 (15, 16) (32% sequence identity, see *SI Text*) shows that R1380 lies within NBD2, ≈10 Å away from the phosphate tail of ATP (Fig. 6*A*). However, neither its side chain nor its backbone contacts the nucleotide. Instead, R1380 appears to interact with a conserved aspartate (D860) in NBD1, which interacts in turn with the γ-phosphate

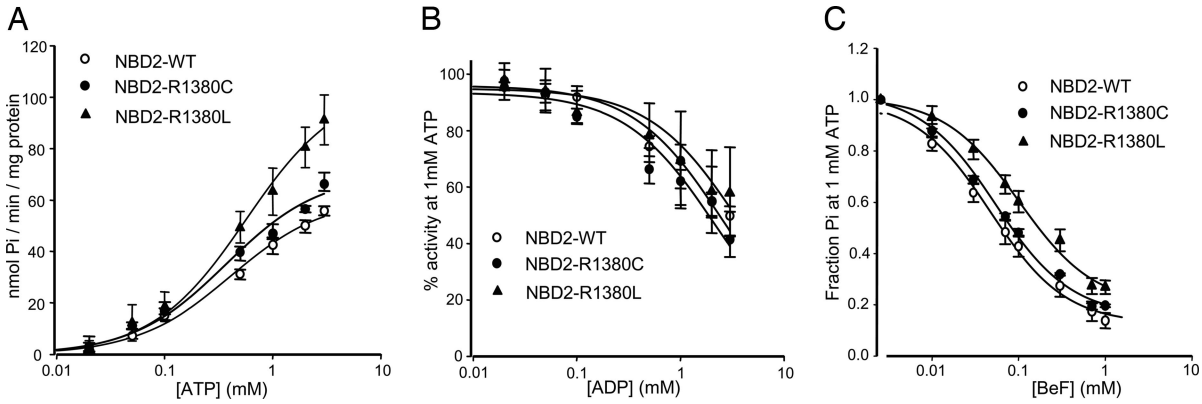

Fig. 2. ATPase activity of SUR1-NBD2 under various conditions. ○, wild-type; ●, R1380C; and ▲, R1380L. (*A*) ATP activity as a function of ATP concentration. (*B*) Concentration dependence of MgADP inhibition of ATPase activity (at 1 mM MgATP). (*C*) Concentration dependence of BeF inhibition of ATPase activity (at 1 mM MgATP).

of ATP (Fig. 6*A*) (13). An aspartate is also present at an equivalent position in the NBD2 homodimer (D1512).

Molecular dynamics simulations were carried out on wild-type and mutant models. To model the posthydrolytic state, MgADP was placed in its binding site and an inorganic phosphate (P_i) was placed where the γ-phosphate of MgATP would be located (see *SI Text*). The simulations show a clear difference in the interaction of P_i in wild-type and mutant models. In the wild-type model, P_i interacts stably with surrounding residues, forming hydrogen bonds with K1385 (during 70% of a 10-ns simulation) and D860 (20%) (Fig. 6*A*). R1380 seems to coordinate D860 through hydrogen bonding of the side chains. In contrast, in the R1380L mutant simulation, P_i quickly loses its interaction with these residues and becomes almost completely hydrated within 6 ns. It forms a weak association with Q1427, but whether this interaction is biologically relevant is less clear (Fig. 6*B*). A more detailed analysis shows that the R1380L mutation does not appear to affect MgADP binding (see *SI Text*), although the simulations are too short to be certain. Overall, the molecular dynamics simulations support the idea that the off-rate for P_i is enhanced by the R1380L mutation. This appears to result from loss of the R1380–D860 interaction, which probably affects association of D860 and P_i.

Discussion

We have identified a mechanism by which mutations in SUR1 give rise to neonatal diabetes: enhanced ATPase activity at NBD2. To our knowledge, this is the first report of a mutation that enhances the ATPase activity of an ABC protein.

ATPase Activity. Mutation of R1380 to C or L increased the ATPase activity of NBD2 of SUR1, as measured by increased P_i production. Both the K_m for MgATP and the K_i for MgADP inhibition were largely unchanged. The fact that MgADP activation was similar for both mutant and wild-type K_{ATP} channels supports the idea that MgADP interaction with NBD2 is unaffected. These data therefore suggest that the observed increase in turnover rate produced by the R1380C and R1380L mutations is primarily a result of an increased hydrolysis of bound MgATP and/or an increased off-rate of P_i (k_3 in Fig. 1*C*). Both mutants bound BeF with lower affinity than wild type. BeF, in combination with MgADP, mimics the γ-phosphate in ATP before hydrolysis and thus traps the cycle in a pseudo-prehydrolytic state. A lower affinity for BeF would be consistent with a lower affinity for P_i and a faster off-rate.

A caveat with these studies is that ATPase activity was measured on isolated NBD2. However, the wild-type data are in good agreement with those we obtained in electrophysiological studies using full-length SUR1. Moreover, mixing NBD2 (wild-type or mutant) with NBD1, to facilitate formation of NBD1–NBD2 heterodimers, gave results qualitatively similar to those from the wild-type or mutant NBD2 homodimers.

In both our model and the crystal structure of the bacterial ABC protein Sav1866 (16), Arg-1380 is ≈10 Å away from the γ-phosphate of ATP. It is therefore unlikely to interact with P_i directly. Our molecular dynamics simulations suggest that the mutation in R1380 disturbs γ-phosphate binding by the loss of the R1380–D860 interaction, which affects D860 association with the phosphate. This possibility is consistent with the functional data.

How does the enhanced rate of ATP hydrolysis at NBD2 favor channel activation? It is now well established that channel activation is facilitated by the presence of MgADP at NBD2, and thus we predict that both mutations will enhance the amount of time spent in the MgADP-bound state. Our results demonstrate that MgADP binding (and transduction) are unaffected, but that ATP hydrolysis (P_i release) is increased. The simplest way to account for these data is to speculate that speeding up the ATPase cycle ensures that more time is spent in the MgADP-bound state and less in the unoccupied (apo) state or MgATP-bound (prehydrolytic state).

In most ABC proteins, R1380 is highly conserved. It has not been implicated previously in binding or catalysis of ATP. Interestingly, when the equivalent residue in SUR2B (R1344) is

Table 1. ATPase activities and kinetic constants

Construct	Turnover rate, s^{-1}	V_{max}, nmol of $P_i \cdot min^{-1} \cdot mg^{-1}$	K_m, mM	*n*
NBD2-WT	0.08 ± 0.002	60.8 ± 1.8	0.41 ± 0.04	4
NBD2-R1380C	0.09 ± 0.004	70.4 ± 3.1*	0.38 ± 0.05	3
NBD2-R1380L	0.13 ± 0.012	104.3 ± 9.9**	0.55 ± 0.09	3

WT, wild type. Values are given as mean ± SEM for *n* separate protein preparations. Significance compared with NBD2-WT: *, $P < 0.05$; **, $P < 0.01$.

Table 2. Inhibition constants for ADP and BeF

Construct	K_i (ADP), mM	K_i (BeF), mM	*n*
NBD2-WT	0.85 ± 0.09	0.02 ± 0.002	4
NBD2-R1380C	0.68 ± 0.11	0.05 ± 0.002*	3
NBD2-R1380L	1.36 ± 0.49	0.10 ± 0.02**	3

Significance compared with NBD2-WT: *, $P < 0.05$; **, $P < 0.01$.

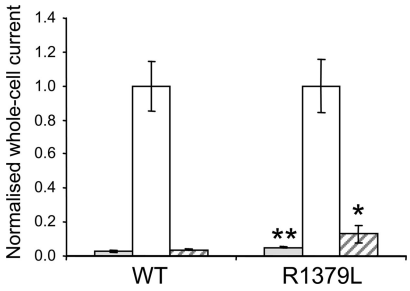

Fig. 3. Mean steady-state whole-cell K_{ATP} currents evoked by a voltage step from −10 to −30 mV before (control, gray bars) and after (white bars) application of 3 mM sodium azide, and in the presence of 3 mM azide plus 0.5 mM tolbutamide (hatched bars) for wild-type channels ($n = 12$) and R1380L channels ($n = 13$). *, $P = 0.05$; **, $P = 0.01$ compared with control (*t* test).

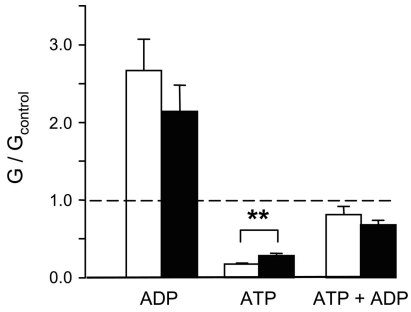

Fig. 5. Mean K_{ATP} currents recorded in the presence of 0.1 mM ADP, 0.1 mM ATP, or 0.1 mM ATP plus 0.1 mM ADP. Currents (*G*) are expressed relative to the mean of the currents recorded in control solution (G_c) before and after application of nucleotide. **, $P < 0.01$.

mutated to alanine, MgADP is no longer able to enhance channel activity preblocked by MgATP (19). Thus the behavior of SUR2B-R1344L channels resembles that of wild-type SUR2A channels. It has therefore been postulated that R1344 may interact with the last 42 amino acids of SUR2, thereby influencing the conformation of the Walker A loop and its functional properties. The fact that the C terminus of SUR1 has a different sequence from both SUR2A and SUR2B may explain why the SUR1-R1380 mutation does not alter MgADP activation.

Channel Activity. The extent of inhibition by MgATP reflects the balance between the inhibitory effect of ATP (via Kir6.2) and the stimulatory effect of MgATP (via SUR1). Any increase in MgATP activation would therefore bias the MgATP concentration–inhibition curve toward higher ATP concentrations. Thus the lower MgATP sensitivity of R1380L channels is consistent with the enhanced rate of MgATP hydrolysis we measure and our suggestion that the dwell time in the MgADP-bound state of the ATPase cycle is increased.

Nucleotide activation of K_{ATP} currents requires Mg^{2+}. Thus if the sole effect of the R1380L mutation were to enhance MgATP hydrolysis at NBD2 of SUR1, there should be no difference in the ATP sensitivity of wild-type and R1380L channels in the absence of Mg^{2+}. Unexpectedly, however, mutant channels showed a lower sensitivity to ATP in the absence of Mg^{2+}. This is not a consequence of an increase in P_o (20), which was unchanged. Therefore the mutation may affect channel activation either by modification of the ATP-binding site on Kir6.2 or by binding of ATP in a Mg-independent fashion to NBD1.

R1380L/C and Neonatal Diabetes. Our data show that mutations at R1380 have modest (<2-fold) effects on the rate of ATP hydrolysis, the ability of ATP to block the K_{ATP} channel, and the resting whole-cell K_{ATP} current. However, because the K_{ATP} channel dominates the membrane potential of the beta cell, even a small increase in K_{ATP} current can cause a hyperpolarization sufficient to inhibit electrical activity and insulin secretion (21). Previous studies of Kir6.2 mutations have shown a good correlation between the magnitude of the K_{ATP} current at physiological levels of MgATP and the severity of the clinical phenotype. It is still too early, however, to say whether such a correlation holds for SUR1 mutations.

Interestingly, some patients with mutations at codon 1380 have transient neonatal diabetes but their relatives have permanent diabetes diagnosed in adulthood (10). This pattern of transient neonatal diabetes in a proband and permanent diabetes diagnosed in childhood or adulthood has been reported in 12 families with 10 different mutations in the *KCNJ11* or *ABCC8* genes (9, 10). Birth weight, a reflection of insulin-mediated growth and thus insulin secretion *in utero*, is reduced to a similar extent whether the patient is diagnosed before 6 months or not (10). These data, together with the similar phenotypes observed between the probands, suggests that genetic modifiers are unlikely to play a large role in phenotypic variability. Rather, our findings imply that K_{ATP} channel mutations have a biphasic course, and that patients diagnosed later in life may have had a period of hyperglycemia that was undetected in the neonatal period.

The *in vitro* response of mutant channels to tolbutamide predicts that patients with an R1380C or R1380L mutation will respond to sulfonylureas. This is indeed the case, because of the nine family members currently studied, five are now treated with

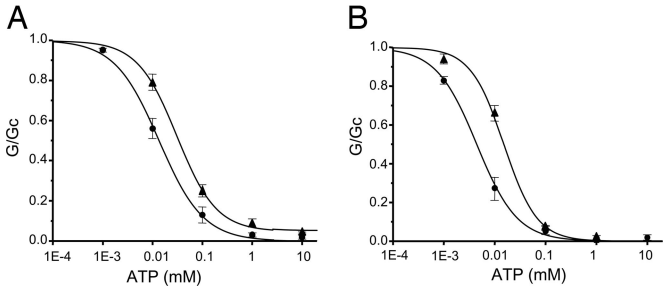

Fig. 4. Mean relationship between ATP concentration and K_{ATP} conductance (*G*), expressed relative to that in the absence of nucleotide (G_c) for wild-type (●) and R1380L (▲) channels. (*A*) In the presence of Mg^{2+}: wild-type channels ($n = 10$) and R1380L channels ($n = 5$). (*B*) In the absence of Mg^{2+}: wild-type channels ($n = 7$) and R1380L channels ($n = 7$).

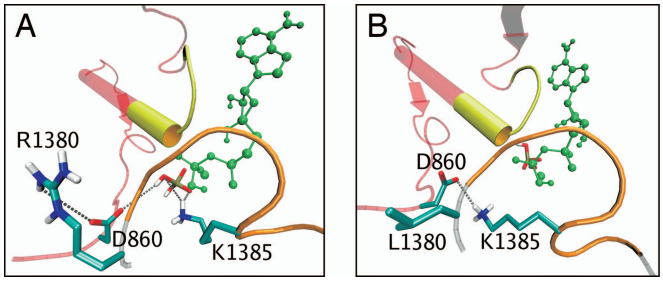

Fig. 6. Wild-type and mutant ATP-binding site 2. (*A*) Homology model of ATP-binding site 2 of wild-type SUR1, indicating the main interactions of the posthydrolytic inorganic phosphate (CPK colors). MgADP is green, the NBD1 backbone is red, the signature sequence of NBD1 is yellow, the NBD2 backbone is gray, and the Walker A domain of NBD2 is orange. (*B*) Mutant model, with the posthydrolytic phosphate unbound. Unlike the wild-type simulation, K1385 hydrogen bonds to D860.

sulfonylureas, whereas four have yet to attempt transfer off insulin (9, 10).

Conclusions. In this study, we have examined the link between mutations in SUR1 and neonatal diabetes, with reference to mutations in the Walker A arginine-1380 of NBD2. We have shown that an increase in K_{ATP} current can be attributed, in part, to an increase in the ATP hydrolysis activity of the nucleotide-binding domains of SUR1.

Materials and Methods

Molecular Genetic Analysis. Genomic DNA was extracted from peripheral leukocytes by using standard procedures. The *ABCC8* gene was amplified and sequenced in probands as described in ref. 10. Results were compared with the published sequence NM_000352.2 with the alternatively spliced residue in exon 17 (L78208, L78224). Compared with the reference sequence used by Babenko *et al*. (9), this includes an additional amino acid. Hence the cysteine mutation at residue 1380 described in this article has previously been reported by Babenko *et al.* (9) as affecting R1379.

NBD2 Mutation and Expression. The C terminus of maltose-binding protein was fused to the N terminus of the second nucleotide-binding domain of rat SUR1 (residues Lys-1319 to Lys-1581) by using the pMal-c2 vector system (New England Biolabs) and expressed as a fusion protein, abbreviated here as NBD2. Site-directed mutagenesis was carried out according to the manufacturer's instructions (QuikChange SDM kit; Stratagene) and confirmed by sequencing. Plasmids were transformed into BL21-CodonPlus *E. coli* cells (Stratagene), and wild-type and mutant proteins were purified as described previously (12). Typical yields were 1.0 mg of protein per liter.

Nucleotide Hydrolysis. ATPase activity was measured with a colorimetric assay for liberated P_i, as described in ref. 22. All assays were performed at 37°C. Details of control experiments are described in ref. 22 and SI Figs. 7 and 8.

Experimental repeats (n) refer to separate protein preparations. All protein preparations were assayed in duplicate. Values are given as mean ± SEM. The Michaelis–Menten equation was fit to concentration–activity relationships and used to obtain the K_m. Turnover rate (nmol of P_i released per second per nmol of protein) was calculated using molecular masses of 87 kDa for MBP-NBD1 and 74 kDa for MBP-NBD2. The IC_{50} for MgADP and BeF inhibition were calculated by fitting the data to the Langmuir equation: $y = B + \{1/[1 + ([I]/IC_{50})]\}$, where y is the ATP hydrolysis rate, IC_{50} is the concentration of inhibitor, I, at half-maximal inhibition, and B is the level of remaining ATPase activity at maximal inhibition (where $B = 0$ for complete inhibition). K_i values were then calculated from the IC_{50} by using the equation for competitive inhibition of Cheng and Prusoff (23): $K_i = IC_{50}/(1 + \{[ATP]/K_m(ATP)\})$.

Electrophysiology. Wild-type or mutant rat SUR1 was coexpressed with human Kir6.2 in *Xenopus* oocytes. Mutant channels (which contain four mutant SUR1 subunits and four wild-type Kir6.2 subunits) are referred to in this paper as R1380L or R1380C channels. Whole-cell currents were recorded by two-electrode voltage clamp (20). Whole-cell currents were normalized to their value in the presence of azide, to take account of difference in expression between different batches of oocytes.

Macroscopic currents were recorded from inside-out membrane patches (20). The pipette solution contained 140 mM KCl, 1.2 mM $MgCl_2$, 2.6 mM $CaCl_2$, and 10 mM Hepes (pH 7.4 with KOH). The intracellular (bath) solution contained 107 mM KCl, 1 mM K_2SO_4, 2 mM $MgCl_2$, 10 mM EGTA, 10 mM Hepes (pH 7.2 with KOH), and MgATP as indicated. ATP concentration–response curves were fit with the Hill equation:

$$\frac{G}{G_c} = a + \frac{(1-a)}{1 + ([ATP]/IC_{50})^h},$$

where [ATP] is the ATP concentration, IC_{50} is the ATP concentration at which inhibition is half maximal, h is the slope factor, a represents the fraction of unblocked current at saturating [ATP], and G is the K_{ATP} conductance. To control for rundown, G_c was taken as the mean of the conductance in control solution before and after ATP application. Single-channel currents were recorded at −60 mV from inside-out patches, as described in ref. 20. All data are given as mean ± SEM. Error bars are shown where they are larger than the symbols. Significance was evaluated by using Student's t test.

Molecular Modeling. A molecular model of the SUR1 NBDs was constructed based on the crystal structure of Sav1866 (16), and molecular dynamics simulations of 9- to 16-ns duration were carried out by using the GROMACS software (24). Full details of the modeling are given in the *SI Text*.

This research was supported by the Wellcome Trust (F.M.A., M.S.P.S., AT.H., and A.-M.P.) and the European Union [F.M.A. and A.T.H., EuroDia-(LSHM-CT-2006-518153)]. F.M.A. is a Royal Society Research Professor. H.d.W. is a Wellcome Trust Training Fellow and is supported by the Wellcome Trust OXION Initiative in Ion Channels and Disease. J.A. is a Wellcome Trust Structural Biology Research Student. A.T.H. is a Wellcome Trust Clinical Research Leave Fellow.

1. Ashcroft FM (2005) *J Clin Invest* 115:2047–2058.
2. Gloyn AL, Pearson ER, Antcliff JF, Proks P, Bruining GJ, Slingerland AS, Howard N, Srinivasan S, Silva JM, Molnes J, *et al*. (2004) *N Engl J Med* 350:1838–1849.
3. Hattersley AT, Ashcroft FM (2005) *Diabetes* 54:2503–2513.
4. Mikhailov MV, Campbell JD, de Wet H, Shimomura K, Zadek B, Collins RF, Sansom MSP, Ford RC, Ashcroft FM (2005) *EMBO J* 24:4166–4175.
5. Tucker SJ, Gribble FM, Zhao C, Trapp S, Ashcroft FM (1997) *Nature* 387:179–183.
6. Nichols CG, Shyng SL, Nestorowicz A, Glaser B, Clement JP, Gonzales G, Aguilar-Bryan L, Permutt MA, Bryan J (1996) *Science* 272:1785–1787.
7. Gribble FM, Tucker SJ, Haug T, Ashcroft FM (1998) *Proc Natl Acad Sci USA* 95:7185–7190.
8. Zingman LV, Alekseev AE, Bienengraeber M, Hodgson D, Karger AB, Dzeja PP, Terzic A (2001) *Neuron* 31:233–245.
9. Babenko AP, Polak M, Cave H, Busiah K, Czernichow P, Scharfmann R, Bryan J, Aguilar-Bryan L, Vaxillaire M, Froguel P (2006) *N Engl J Med* 355:456–466.
10. Flanagan SE, Patch A-M, Mackay DJ, Edghill EL, Gloyn AL, Robinson D, Shield JP, Temple K, Ellard S, Hattersley AT (2007) *Diabetes* 56:1930–1937.
11. Masia R, Enkvetchakul D, Nichols CG (2005) *J Mol Cell Cardiol* 39:491–501.
12. de Wet H, Mikhailov MV, Fotinou C, Dreger M, Craig TJ, Vénien-Bryan C, Ashcroft FM (2007) *FEBS J* 274:3532–3544.
13. Campbell JD, Proks P, Lippiat JD, Sansom MS, Ashcroft FM (2004) *Diabetes* 53:S123–S127.
14. Locher KP (2004) *Curr Opin Struct Biol* 14:426–431.
15. Dawson RJ, Locher KP (2006) *Nature* 443:156–157.
16. Dawson RJ, Locher KP (2007) *FEBS Lett* 581:935–938.
17. Werber MM, Peyser YM, Muhlrad A (1992) Biochemistry 31:7190–7197.
18. Proks P, Shimomura K, Craig TJ, de Wet H, Girard CAJ, Ashcroft FM (2007) *Hum Mol Genet* 16:2011–2019.
19. Matsushita K, Kinoshita K, Matsuoka T, Fujita A, Fujikado T, Tano Y, Nakamura H, Kurachi Y (2002) *Circ Res* 90:554–561.
20. Proks P, Antcliff JF, Lippiat J, Gloyn AL, Hattersley AT, Ashcroft FM (2004) *Proc Natl Acad Sci USA* 101:17539–17544.
21. Tarasov AI, Welters HJ, Senkel S, Ryffel GU, Hattersley AT, Morgan NG, Ashcroft FM (2006) *Diabetes* 55:3075–3082.
22. Chifflet S, Torriglia A, Chiesa R, Tolosa S (1988) *Anal Biochem* 168:1–4.
23. Cheng Y, Prusoff WH (1973) *Biochem Pharmacol* 22:3099–3108.
24. Berendsen HJC, van der Spoel D, van Drunen R (1995) *Comput Phys Commun* 91:43–56.